BProbeM: a tool to measure matrix geometries

Timon Salar Gutleb

University of Vienna

ESI Workshop: Matrix Models for Noncommutative Geometry and String Theory

July 9th, 2018

Overview

1. Extracting semi-classical geometry from matrix models

2. A quick live demonstration

Extracting semi-classical geometry from matrix models

Preliminary Remarks (I)

Given some matrix geometry $A^\mu \in End(\mathcal{H}_N)$, how can we extract an underlying semi-classical Poisson-manifold?

Measuring finite Quantum Geometries via Quasi-Coherent States

Lukas Schneiderbauer[1], Harold C. Steinacker[2]

Faculty of Physics, University of Vienna
Boltzmanngasse 5, A-1090 Vienna, Austria

Abstract

We develop a systematic approach to determine and measure numerically the geometry of generic quantum or "fuzzy" geometries realized by a set of finite-dimensional hermitian matrices. The method is designed to recover the semi-classical limit of quantized symplectic spaces embedded in $\mathbb{R}^d$ including the well-known examples of fuzzy spaces, but it applies much more generally. The central tool is provided by quasi-coherent states,

Preliminary Remarks (II)

Ideas based in part on previous work by

PHYSICAL REVIEW D **86,** 086001 (2012)

Matrix embeddings on flat $\mathbb{R}^3$ and the geometry of membranes

David Berenstein[1,2] and Eric Dzienkowski[1]

[1]*Department of Physics, University of California at Santa Barbara, Santa Barbara, California 93106, USA*
[2]*Kavli Institute for Theoretical Physics, Santa Barbara, California 93106, USA*
(Received 7 May 2012; published 1 October 2012)

We show that given three Hermitian matrices, what one could call a fuzzy representation of a membrane, there is a well-defined procedure to define a set of oriented Riemann surfaces embedded in $\mathbb{R}^3$ using an index function defined for points in $\mathbb{R}^3$ that is constructed from the three matrices and the point. The set of surfaces is covariant under rotations, dilatations and translation operations on $\mathbb{R}^3$; it is additive on direct sums; and the orientation of the surfaces is reversed by complex conjugation of the matrices. The index we build is closely related to the Hanany-Witten effect. We also show that the surfaces carry information of a line bundle with connection on them. We discuss applications of these ideas to the study of holographic matrix models and black hole dynamics.

DOI: 10.1103/PhysRevD.86.086001

Extracting geometry from matrix models (I)

(Matrix Laplace operator) Given a point-probed background $\mathfrak{X} = \begin{pmatrix} A^\mu & 0 \\ 0 & x^\mu \end{pmatrix}$ with $\mu = 0, ..., d$, we define the *matrix Laplace operator* on $\mathfrak{X}$ as a map

$$\Box_{\mathfrak{X}} : \mathrm{Mat}_{m+1}(\mathbb{C}) \to \mathrm{Mat}_{m+1}(\mathbb{C})$$

$$\Box_{\mathfrak{X}} := \sum_{\mu=1}^{d} [\mathfrak{X}^\mu, [\mathfrak{X}^\mu, .]] \,.$$

It acts on $End(\mathcal{H}_m \oplus \mathbb{C}) = End(\mathcal{H}_m) \oplus \mathcal{H}_m \oplus \mathcal{H}_m^T \oplus \mathbb{C}$, where the off-block-diagonal parts $\mathcal{H}_m \oplus \mathcal{H}_m^T$ represent the string connecting the matrix set A^μ to the zero-dimensional point probe x^μ.

$$\Box_{\mathfrak{X}}\Phi = \sum_{\mu=1}^{d} [\mathfrak{X}^\mu, [\mathfrak{X}^\mu, \Phi]] = \begin{pmatrix} \begin{matrix} 0 & \dots & 0 \\ \vdots & \ddots & \vdots \\ 0 & \dots & 0 \end{matrix} & \sum_{\mu=1}^{d} (A^\mu - x^\mu)^2 \, |\phi\rangle \\ \langle\phi| \sum_{\mu=1}^{d} (A^\mu - x^\mu)^2 & 0 \end{pmatrix}$$

Extracting geometry from matrix models (II)

(Point-probe Laplace operator)

$$\square_x := \sum_{\mu=1}^{d} (A^\mu - x^\mu)^2 \,. \tag{1.1}$$

Finding quasi-coherent states can be reduced to an eigenvalue problem.

$$\langle\phi|\,\square_x\,|\phi\rangle = \left|\vec{x} - \langle\Psi|\,\vec{A}\,|\Psi\rangle\right|^2 + \sum_{\mu=1}^{d}(\Delta_\Psi A^\mu)^2 =: E(\vec{x}) \tag{1.2}$$

Extracting geometry from matrix models (III)

(Quasi-coherent states) We call a state $|\Psi\rangle \in \mathcal{H}_N$ a *quasi-coherent state* at $\vec{x} \in \mathbb{R}^d$ if it holds that the displacement energy $E(\vec{x})$ is minimal at $\vec{x}$, where we define:

$$E(\vec{x}) := |\vec{x} - \langle A \rangle|^2 + \delta(\Psi)$$

With $\vec{x} \in \mathbb{R}^d$ a point in target space. This can be restated as an eigenvalue problem, making it approachable using numerical tools.

Sketch of the scanning algorithm

Given a local minimum x_0 of the displacement energy function, the Hessian at x_0 should show a hierarchy of small and large eigenvalues. Selecting x_0 and an appropriate stepsize length $|\epsilon|$ are the initialization steps and require manual attention. After this we iterate over the following steps:

- Collect all currently collected local minima into a set M.
- Obtain new point candidates from the points x_i in M by performing $x_i + \epsilon_i$ where ϵ_i is a vector of stepsize length $|\epsilon|$ in the direction corresponding to an eigenvector of the Hessian matrix corresponding to the small eigenvalues.
- Replace the candidate point set with its corresponding expectation values using the quasi coherent states at the respective point, i.e. $\langle\psi_{x_i}|\, x_i \,|\psi_{x_i}\rangle$.

The resulting set M gives a semi-classical approximation of the quantized manifold.

An example of this procedure: Fuzzy 2-sphere

The fuzzy 2-sphere, denoted S_N^2, is defined by three matrices $A^i, i = 1, 2, 3$ satisfying a commutation relation:

$$[A^a, A^b] = i\frac{2}{\sqrt{N^2 - 1}}\epsilon_{abc}A^c. \tag{1.3}$$

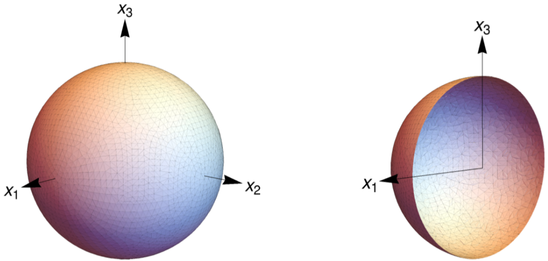

(a) Full picture of $\mathscr{M} = S_{10}^2$.

(b) A cut through the $x_1 - x_3$-plane to show that there are no points inside.

Figure 8.1: Visualization of the semi-classical limit of the fuzzy sphere S_N^2 constructed from S_{10}^2.

More examples

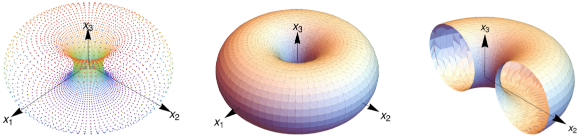

(a) The raw point cloud which is generated by the numerical procedure.

(b) A polygon mesh generated from the point cloud in figure 8.2a.

(c) A cut through the torus to show that it is hollow.

Figure 8.2: Visualization of the semi-classical limit of the fuzzy torus T_N^2 constructed from T_{20}^2.

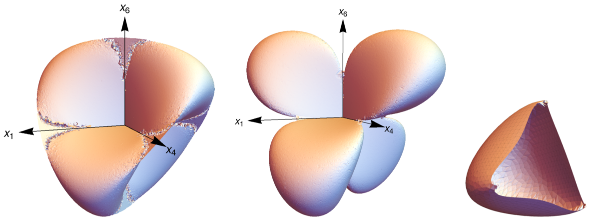

(a) Laplace coherent states of $\Pi(\mathbb{C}P_{30}^2)$.

(b) Dirac coherent states of $\Pi(\mathbb{C}P_3^2)$.

(c) A cut through one of the vaults of 8.3b to show that it is hollow.

Figure 8.3: Visualization of numerically obtained coherent states of squashed $\mathbb{C}P_N^2$.

A quick live demonstration

Wolfram Mathematica implementation

- The original package is available at:
  https://github.com/lschneiderbauer/BProbe

- An updated fork that is being maintained is available at:
  https://github.com/TSGut/BProbeM